Single Board Computer-Based Control System for Reconfigurable Intelligent Surface Applications

M. Tech. Thesis

By

Nikhil Ranjan

DEPARTMENT OF ELECTRICAL ENGINEERING

INDIAN INSTITUTE OF TECHNOLOGY INDORE

May 2025

Single Board Computer-Based Control System for Reconfigurable Intelligent Surface Applications

A THESIS

Submitted in partial fulfillment of the
requirements for the award of the degree
of
Master of Technology

by
Nikhil Ranjan

DEPARTMENT OF ELECTRICAL ENGINEERING
INDIAN INSTITUTE OF TECHNOLOGY INDORE
May 2025

INDIAN INSTITUTE OF TECHNOLOGY INDORE

CANDIDATE'S DECLARATION

I hereby certify that the work which is being presented in the thesis entitled **Single Board Computer-Based Control System for Reconfigurable Intelligent Surface Application** in the partial fulfillment of the requirements for the award of the degree of **MASTER OF TECHNOLOGY** and submitted in the **DEPARTMENT OF ELECTRICAL ENGINEERING, Indian Institute of Technology Indore**, is an authentic record of my own work carried out during the time period from July 2023 to May 2025 under the supervision of Dr. Saptarshi Ghosh, Assistant Professor, IIT Indore.

The matter presented in this thesis has not been submitted by me for the award of any other degree of this or any other institute.

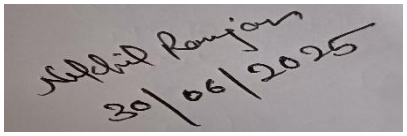

Signature of the student with date
Nikhil Ranjan

This is to certify that the above statement made by the candidate is correct to the best of my/our knowledge.

28-06-2025
DR. SAPTARSHI GHOSH
Signature of the Supervisor of MTech. thesis (with date)

Mr. Nikhil Ranjan has successfully given his M. Tech. Oral Examination held on **07/05/2025.**

Signature of Supervisor
Date: 28-06-2025

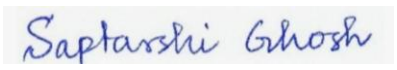

Signature of Convener, DPGC-EE
Date: 28-06-2025

ACKNOWLEDGEMENTS

I would also like to thank all the PSPC members, Dr. Prabhat Kumar Upadhyay, Dr Appina Balasubramanyam, Dr Summit Gautam, and Dr Dibbendu Roy for their questions and suggestions which have motivated me to work more diligently towards my research work. I would like to thank IIT Indore for all the facilities and the Ministry of Education for financial support.

A special gratitude to my senior PhD scholar Deepak Kaushik for his expert guidance and sharing practical knowledge with me. I also want to thank my lab mates Akhila Gouda, P Megh Sainadh, Munna Aziz, Deepak, Akash Ahirwar, and Goundla Sricharni for their help, cooperation, and encouragement. I would like to thank all my friends who made my journey at IIT Indore an indelible and gratifying experience.

Finally, my heartfelt gratitude towards my family for their tireless love and support and their unceasing encouragement and moral support throughout this journey.

Nikhil Ranjan

Abstract

In today's wireless communication landscape, there is an ever-growing need for higher data transmission rates to support the rising demand for data-heavy applications such as HD video streaming, online gaming, and real-time video conferencing. These applications rely on fast and dependable wireless connectivity to operate efficiently. While the demand for wireless services continues to escalate, the spectrum available for communication remains limited. Consequently, network providers are compelled to utilize the existing spectrum more effectively to accommodate a greater number of users and bandwidth-demanding applications.

One intuitive solution is to shift towards higher frequency bands, which offer greater bandwidth availability. However, this approach comes with the trade-off of reduced coverage range, necessitating smaller cell sizes and the deployment of additional base stations—ultimately increasing infrastructure costs. Therefore, addressing user demands in modern wireless networks requires innovative and strategic solutions to overcome these limitations.

Recently, Reconfigurable Intelligent Surfaces (RIS) have emerged as a promising solution. RIS is composed of nearly passive components that only require activation through applied voltage and lack traditional RF chains. Rather than modifying endpoints of the network, RIS technology alters the wireless propagation environment itself. RIS is anticipated to offer several advantages: (1) extended signal coverage, (2) lowered infrastructure expenses, (3) enhanced energy efficiency, and (4) increased network throughput.

This thesis introduces the first in-house developed RIS prototype consisting of 4096 individual elements operating in the Sub-6 GHz frequency band. The chosen operating frequency is approximately 3.75 GHz, aligning with

current 5G frequency bands. Each RIS unit is equipped with Positive Intrinsic-Negative (PIN) diodes that toggle between two distinct phase states. Individual control of each element allows the RIS to function effectively in the near-field and enables accurate channel estimation.

The prototype demonstrates an operational power consumption ranging between 12 to 15 watts and achieves beam switching speeds of up to 15 mega symbols per second. The thesis explores the application of RIS in wireless communication systems, where the RIS can dynamically steer the beams in real-time and improve the signal quality for non-line-of-sight (NLoS) conditions, as demonstrated using an OFDM-based setup. In addition, the proposed control system-based RIS device have significant potential in healthcare applications in detecting vital signs, such as heart rate and respiration. Additionally, investigations into the electromagnetic field (E-field) exposure around a human head model reveal that RIS can lower E-field intensity by dynamically adjusting its reflective properties. Thus, the thesis aims to examine and validate the practical utility of RIS technology in wireless communication, and opens up its possible applications in healthcare domains, as well.

TABLE OF CONTENT

TABLE OF FIGURE

LIST OF TABLES

ACRONYMS

BER – Bit Error Rate

BW - Bandwidth

DAC – Digital-to-Analog convertor

EM – Electromagnetic

FPGA – Field Programmable Gate Array

HFSS – High Frequency Structure Simulator

ICs – Integrated Circuits

MIMO – Multiple Input Multiple Output

NLoS – Non-line of sight

PCB – Printed Circuit Board

RCS – Radar Cross section

RF – Radio Frequency

RIS – Reconfigurable Intelligent surface

SE – Spectral efficiency

UAV – Unmanned Aerial Vehicles

UDNs – Ultra Dense Networks

UDS – Advanced Design System

UHD – Ultra High Definition

USRP – Universal Software Radio Peripheral

VoIP – Voice over Internet protocol

XR – Extended Reality

Chapter 1

Introduction

1.1. Background and Motivation:

Over the past 40 years, mobile communication has evolved through five generations, each emerging roughly every decade with better technologies and features. Before the 1980s, 0G networks like walkie-talkies allowed basic radio communication. In the 1980s, 1G introduced analog mobile voice calls. Then came 2G, which used digital signals and added SMS. The 3G era brought mobile internet, MMS, video calls, and mobile TV. 4G (LTE) further improved speed, enabling VoIP, UHD video, and online gaming.

Currently, 5G is being deployed worldwide. It supports advanced applications like IoT, autonomous vehicles, and virtual/augmented reality, mainly due to technologies like network softwarization. Research is now focused on Beyond 5G (B5G) and 6G, which aim to deliver extremely high data rates, ultra-low latency, and highly reliable connections. These networks will support emerging technologies like Extended Reality (XR), holographic telepresence, drones, smart grids, and Industry 5.0, all of which require faster, smarter, and more efficient networks.

To achieve this, key improvements in future wireless systems will include better spectral efficiency using cell-free Massive MIMO, more base stations through Ultra-Dense Networks (UDNs), and use of high-frequency bands like mm Wave. A major feature of 6G will be Integrated Sensing and Communication (ISAC), which combines communication and sensing for applications such as gesture recognition, smart healthcare, and precise positioning. Technologies

like Wi-Fi, mm Wave, and Terahertz are already used in sensing, and integrating them with cellular networks could help build intelligent environments like smart homes and hospitals

1.2. Statement of the Problem:

Using Massive MIMO and more base stations improves network speed but is very costly and increases system load. High frequencies like mm Wave and THz offer faster data but have poor range and can't pass through walls or obstacles well. THz devices also need special, expensive hardware that uses a lot of power and can overheat.

Sensing technologies like Wi-Fi or mm Wave use different systems and can't easily work with mobile networks. Most sensing tests are done in simple lab setups and don’t work well in real environments. But cellular sensing can turn mobile towers and phones into sensors with wide coverage. To work well, though, the signals must be aimed accurately using phased arrays, which use more energy and don’t work well when there’s no direct line of sight

1.3. Aim and Goal of the Thesis:

This research is focused on developing a unified solution that can support both wireless communication and RF sensing in non-line-of-sight (NLoS) environments. High-frequency communication systems often rely on relays or repeaters to extend coverage, while RF sensing systems require minimal background reflections and low-noise conditions. Additionally, both types of systems necessitate the capability to track multiple users simultaneously, typically using beam steering techniques.

A promising innovation addressing these challenges is the Reconfigurable Intelligent Surface (RIS), a technology capable of dynamically altering the behavior of incident electromagnetic (EM) waves to achieve high signal gain, beam steering, or beam focusing. Accordingly, the primary goals of this thesis are as follows:

1. To design and implement a real-time RIS prototype suitable for 5G systems, operating around the 3.6 GHz frequency band.
2. To investigate the applicability of RIS in different domains, particularly in wireless communication and healthcare.
3. To assess the performance of current beam steering techniques when applied to RIS-enabled systems.
4. To examine and propose methods for managing 5G signal exposure using RIS technology.

1.4. Thesis Contribution:

This work makes two key contributions in the area of Reconfigurable Intelligent Surfaces (RIS): first, it involves building a hardware testbed for RIS, and second, it shows how RIS can improve wireless communication performance. Three different capabilities of the developed RIS have been experimentally demonstrated, as follows:

1. RIS enabled beam steering in far field.
2. RIS support beam splitting.
3. RIS support multi-user beam

Chapter 2

Literature Review

2.1. Background:

The upcoming 6G networks aim to deliver faster data and lower latency by using advanced technologies like Massive MIMO, mm Wave, and Terahertz (THz) frequencies. THz bands can solve current issues like limited spectrum and high data demand, and even support communication between tiny devices like nanomachines. However, high signal loss at these frequencies, especially over distance and in the presence of air molecules—makes reliable communication difficult.

To overcome these issues, Reconfigurable Intelligent Surfaces (RIS) have been introduced. RIS can reflect wireless signals in specific directions to boost strength and coverage. They offer a low-cost and energy-saving solution for improving wireless networks. Still, RIS faces challenges like limited range, complex control systems, and unpredictable environments. This thesis explores recent research, key functions, and working examples of RIS technology.

2.2. Introduction:

Electromagnetics studies how electric and magnetic fields behave over space and time. Based on how the waves change with time, the electromagnetic (EM) spectrum is divided into different regions—such as radio waves, microwaves, millimeter waves, infrared, visible light, ultraviolet, X-rays, and gamma rays. The way EM waves behave in space, especially when they interact with materials

like metals and insulators, leads to effects such as reflection, refraction, diffraction, dispersion, and absorption.

These natural behaviors have inspired many scientific developments. For example, light bending in water due to refraction makes a spoon appear bent, and dispersion of light through water droplets creates rainbows. Total internal reflection in glass led to the invention of optical fiber used in high-speed communication. At lower frequencies like radio and microwave, studying wave reflection from metal surfaces helped create parabolic dish antennas. These reflective surfaces—whether metallic or dielectric—continue to play a key role in modern wireless communication systems.

2.3. Reconfigurable Intelligent Surface:

In recent years, there has been a growing interest in specially designed metallic surfaces called metasurfaces. Unlike regular metal sheets, metasurfaces are engineered with tiny, carefully arranged elements that give them unique electromagnetic properties not found in natural materials. This new area of study is known as "Surface Electromagnetics."

Traditional metal surfaces reflect signals uniformly with constant impedance. However, textured metallic surfaces—made of small elements spaced closer than the signal wavelength—can be designed to behave like inductors or capacitors. This allows control over how much the signal's phase is delayed or advanced, up to 360°, by tuning the surface impedance.

Reconfigurable Intelligent Surfaces (RIS) are an advanced form of these texture surfaces. An RIS is made of many small elements that

act like tiny reflectors. Each element can be controlled to reflect signals in a specific way, changing the overall direction or shape of the reflected signal. This control is done in real time using software. Unlike traditional reflect arrays used in satellites, RIS can adapt to different functions like signal steering, focusing, or scattering, and even perform special tasks like frequency mixing or polarization conversion.

The development of RIS has evolved over time. Initially, these surfaces were simple and designed for fixed frequency and direction. Later, with the use of active components, RIS could be tuned for different frequencies and functions. More recently, digital programmable surfaces were introduced to simplify control and reduce processing load. With the help of AI and machine learning, RIS can now become even smarter and more efficient, enabling dynamic and intelligent control in future wireless communication systems.

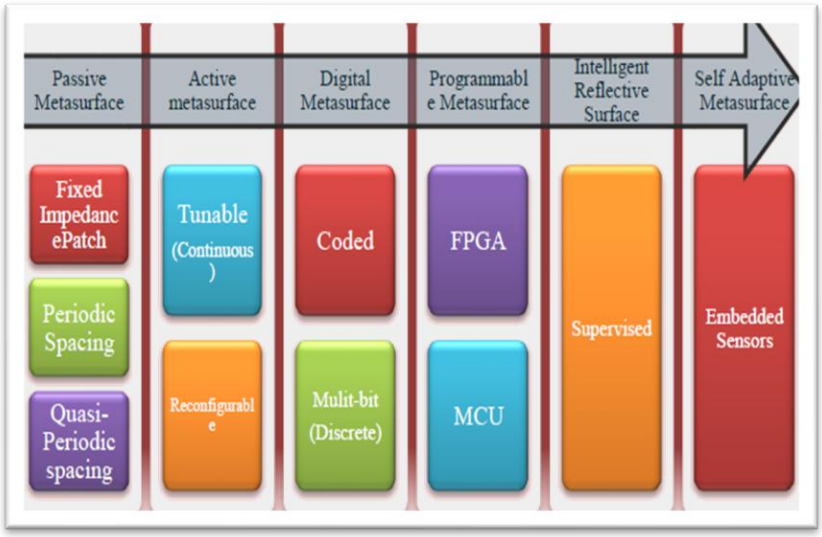

Figure 2.2 Evolution of the RIS

2.4. Tuning Mechanisms:

The reconfigurability of a reflective surface, like an RIS, depend on how we control the phase and strength of the signals reflected by its small units (called unit cells). Two common methods for this are analog and digital control.

In analog control, components like varactor diodes, BST (Barium Strontium Titanate) capacitors, and liquid crystals are used. These can finely adjust the phase of the reflected signal. However, BST capacitors and liquid crystals are hard to find and need complex manufacturing steps. Varactor diodes are easier to find but need high voltages and special DAC chips to control them.

Digital control is simpler and uses components like PIN diodes, MEMS switches, or relays. These are more readily available. FETs (field-effect transistors) are not preferred for high-frequency switching because they lose more signal power. Relay switches are too large for dense RIS designs. PIN diodes are most commonly used because they are small, simple (two terminals), and have low signal loss**.**

2.5. Functionalities of RIS:

While a basic reconfigurable surface may be limited to a single function like beam steering, a significant advantage of RIS technology lies in its ability to perform multiple functions. This multifunctionality is achieved by applying various coding schemes that enable precise control over electromagnetic (EM) wave propagation. The following sections outline some of the core capabilities enabled by this approach.

2.5.1. Beam Focusing:

One exciting feature of RIS is its ability to focus signals in the far field. For example, a RIS panel that is 1. square meters in size and operates at 3.6 GHz can focus signals. Unlike a mirror, which just reflects waves in a flat direction, a RIS works more like a lens. Each small part of the RIS can change the phase of the signal it reflects. Together, these tiny adjustments help focus the signal at a specific point in space, based on desired direction and height (azimuth and elevation)

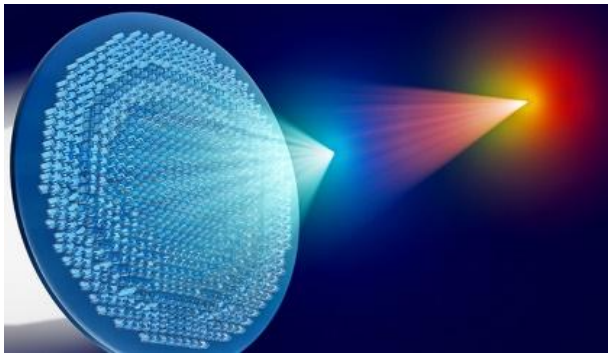

Figure 3.2 Beam focusing

2.5.2. Beam steering:

RIS (Reconfigurable Intelligent Surface) can also change the direction of signals, which is known as **beam steering**. This can help send signals directly toward a user or device, even if they are moving around.

It works like a smart mirror that can bend and aim the signal wherever needed. By adjusting each tiny part of the surface, RIS can guide the signal in the right direction. This makes the connection stronger and more stable, especially in places where

signals get blocked by walls or other objects. Beam steering helps keep users connected, no matter where they go

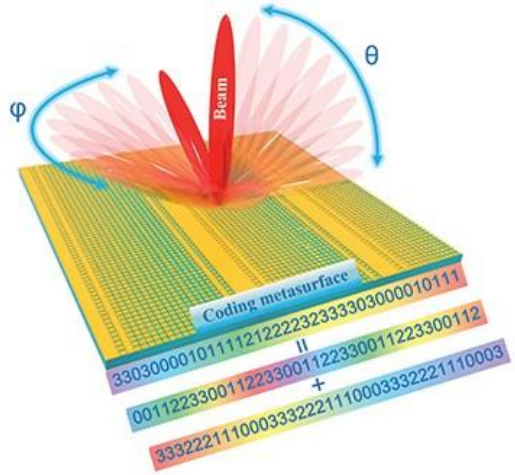

Figure 2.4 *Beam steering*

2.5.3. Beam Scattering/diffusion:

Since World War II, researchers have worked on making objects invisible to radar by reducing their Radar Cross Section (RCS). The goal is to design surfaces that either absorb or scatter electromagnetic (EM) waves so they are not detected by enemy radar.

Traditionally, this is done using special materials or shaping the object to reduce reflections. Some surfaces use fixed patterns, like chessboard designs or random coding sequences, to scatter signals. But once these surfaces are made, the patterns can’t be changed. With RIS technology, however, we can now control and change these patterns in real-time using software. This makes RIS a more flexible and effective solution for RCS reduction.

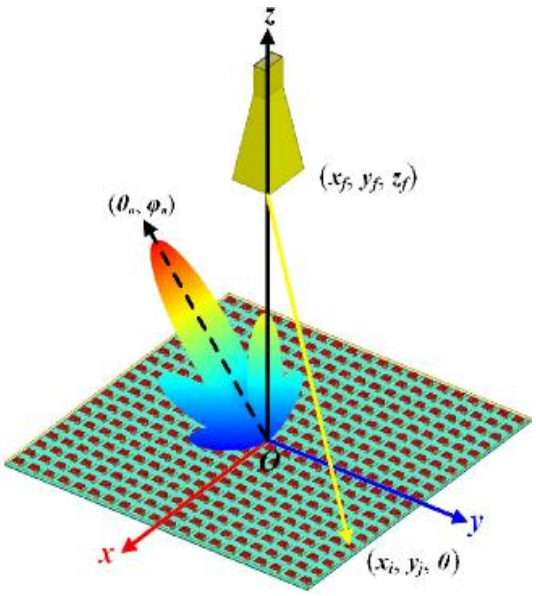

Figure 2.5 Scattering

2.5.4. Multi-beam generation:

In current antenna systems, beam steering is done at the transmitter using special circuits that direct the signal toward users. When many users are present, it's better to generate multiple beams to serve them at once. This is usually done with phased array antennas, which can create one or more strong beams. However, they need many expensive parts like RF chains, phase shifters, and power amplifiers.

To lower the cost, some systems use passive reflectors, like parabolic dishes, to reflect beams created by low-power phased arrays. These work well for fixed locations like satellite ground stations, but they can't follow moving users. RIS offers a smarter, low-cost solution. It doesn't need power-hungry components and can generate multiple beams by adjusting how each small part of the surface reflects signals. By changing the

phase or strength of the reflections from each element, RIS can steer or split beams toward different users, acting like a beam splitter that sends varying amounts of power in different directions.

2.6. RIS vs Relay Station:

Reconfigurable intelligent surface (RIS) can be compared with relay stations, which are commonly used to extend communication range. A relay station receives signals, processes them, amplifies them, and then sends them out again. However, this comes with drawbacks. Relays need complex signal processing circuits and power amplifiers, which makes them expensive and power-hungry. They also require a constant power supply to function.

Relays typically work in two modes: half-duplex (sending and receiving signals at different times) and full-duplex (sending and receiving at the same time). Half-duplex is less efficient, while full-duplex suffers from interference problems, which again need complicated circuits to fix. On the other hand, RIS doesn't need any transmitter or amplifier. It reflects signals by smartly adjusting the surface elements and works in full-duplex mode naturally. Studies have shown that RIS can require less transmission power than traditional relays like Decode-and-Forward (DF) and can be more energy efficient than Amplify-and-Forward (AF) relays. However, real-world experiments comparing them are still ongoing.

2.7. Coded and Programmable RIS:

Traditional metamaterials are usually designed by changing the overall material properties, like permeability and permittivity. These

are called analogue metamaterials because they affect the entire surface in a uniform or non-uniform way. In contrast, coded meta surfaces work differently. Each small unit cell is assigned a digital code, such as 0 or 1, to control how it reflects waves. For example, a simple 1-bit system changes the phase of reflected waves to either 0° or 180°, depending on whether the code is 0 or 1.

When we want finer control and higher performance, we can increase the number of bits, such as using 2-bit or 3-bit coding. This allows more phase options, but it also increases the number of wires needed to control each unit cell. For instance, a 3-bit system needs three wires per cell, which makes the design more complex, especially for large surfaces or high-frequency applications. Research has shown that 2-bit coding offers a good balance between performance and complexity. To further improve without increasing physical complexity, a time-based approach has been proposed where only 2-bit coding is used, but the phase is changed over time. This method can simulate up to 4 phase levels, reducing the need for complicated hardware.

Chapter 3

Design and Fabrication of the RIS

3.1. Introduction:

The insights discussed in the preceding chapter lay the foundation for the practical realization of RIS, including the unit cell configuration and optimal inter-element spacing. This chapter focuses on the design and integration of the control circuitry with the RF (radio frequency) layer.

The development of a functional RIS system requires expertise across several disciplines, such as electromagnetics, wireless communication, embedded systems, and computer science. Current research efforts span these diverse fields. In the proposed work, the RIS architecture is divided into three primary components, as illustrated in Figure 3.1: the electromagnetic (EM) layer, the DC control layer, and the controller module. Each of these layers will be independently modeled, integrated, and refined to achieve complete hardware functionality. The subsequent sections provide a brief overview of the individual components within each layer.

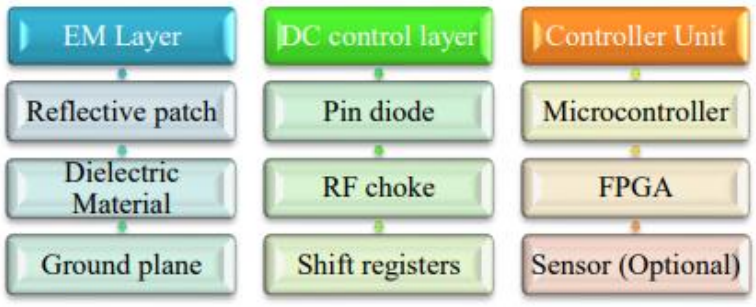

Figure 3.1Proposed hardware layout of the RIS

3.2. Control Circuit Layout:

In Figure 3.2, it can be seen that the operation of diodes is controlled through the shift registers with the cathode connected to the ground. The 74HC/HCT595 is a widely used high-speed CMOS chip that works as an 8-bit serial-in, parallel-out shift register. It allows data to be entered serially and then outputted either serially or in parallel. The chip consists of two main parts: a shift registers and a storage register, each controlled by its own clock signal. One of its useful features is the 3-state output, which allows multiple chips to share the same output lines without interference. It also has a direct clear function to reset the shift register. The chip can operate at frequencies up to 100 MHz and includes protection against electrostatic discharge (ESD), making it reliable in different environments. The 74HC595 is especially useful in applications where we need to convert serial data into parallel output, such as in LED displays or remote-controlled devices

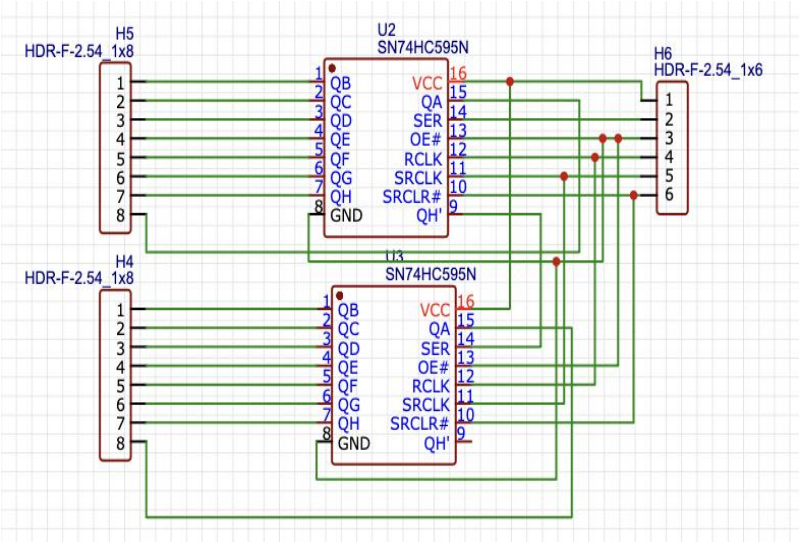

Figure 3.2 Schematic layout of the cascade diode controller circuit

3.2.1 Design of PCB:

The below images illustrate the step-by-step design process of a custom PCB layout created for interfacing two 74HC595 shift registers. Fig 3.3 shows the basic component placement on the PCB design software, where two DIP-16 ICs (U2 and U3) and header pins (H4, H5, and H6) are arranged for proper connectivity. Fig 3.4 provides a 3D view of the PCB with the components placed, giving a realistic representation of the final hardware. Fig 3.5 represents the final PCB routing, where red and blue lines indicate the top and bottom copper layers for signal traces. This board was designed to simplify the control of multiple output devices using fewer FPGA GPIOs by serial-to-parallel data conversion through the 74HC595 ICs. The design also helps in neatly organizing the connections, making it easier to implement and troubleshoot in real-time hardware experiments.

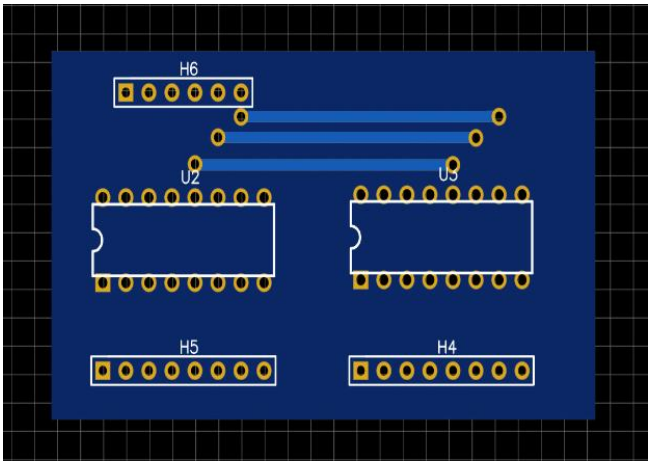

Figure 3.3 3-D Design of PCB

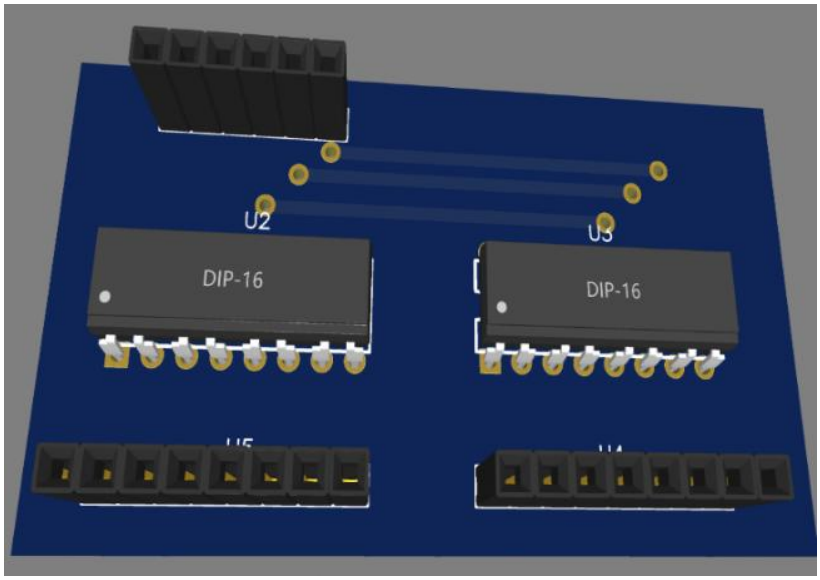

Figure 3.4 3D Design of PCB

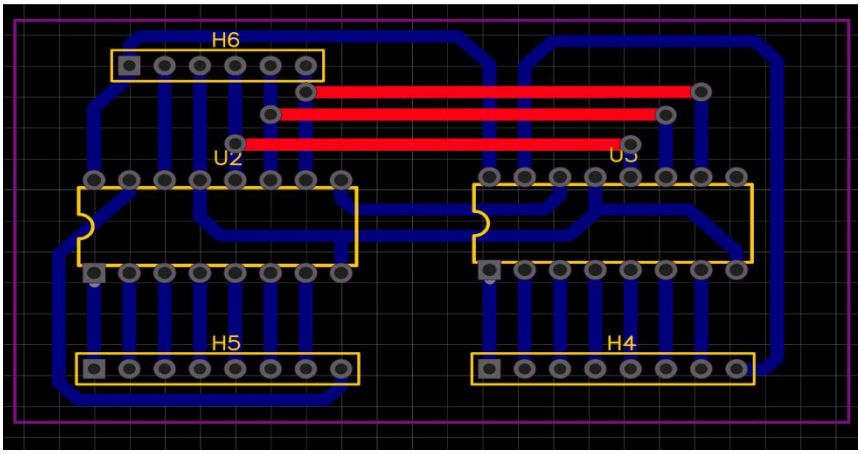

Figure3.6 PCB Layout

3.2.2 Fabricated Custom PCB for Shift Register Interfacing

Fig 3.6 shows the final fabricated version of the custom-designed PCB used for connecting two 74HC595 shift register ICs. The black IC sockets (DIP-16) are mounted to allow easy insertion and replacement of the shift register chips without soldering them directly. Multiple female header pins are also

soldered to provide convenient interfacing with external microcontrollers or FPGA boards. Some manual wire connections (yellow and green) have been made on the PCB to correct or establish crucial signal paths, which were either not routed in the PCB design or needed post-fabrication adjustments. This setup was created to expand the number of controllable outputs using fewer control lines efficiently

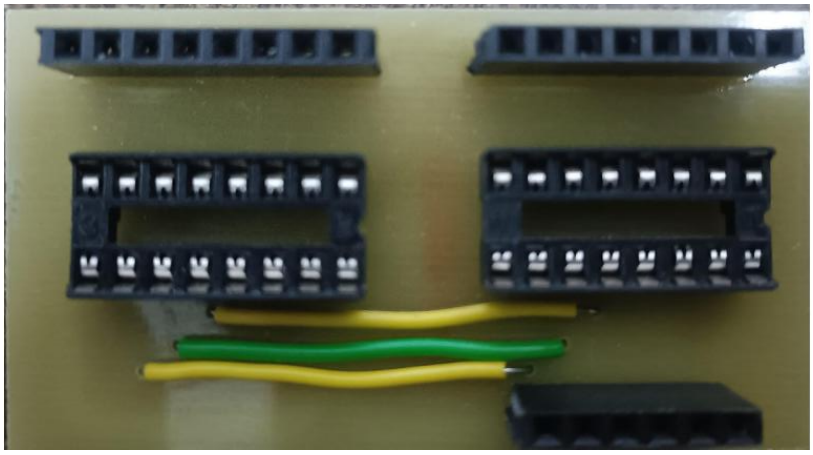

Figure 3.7 Fabricated PCB

3.3. Controller of RIS:

Fig 3.7 shows a setup where LEDs are connected to a breadboard and controlled by an FPGA development board. Each LED is wired to different output pins of the FPGA using yellow jumper wires. This setup demonstrates how an FPGA can be used to control the ON/OFF states of LEDs, similar to how PIN diodes are controlled in an RIS. Just like PIN diodes can be turned on or off to control the reflection phase of EM waves, here the Basys3 FPGA board controls each LED's state through digital signals, showing the concept of programmable control in a simple and visual way. Fig. 3.8 shows the control of LED by FPGA.

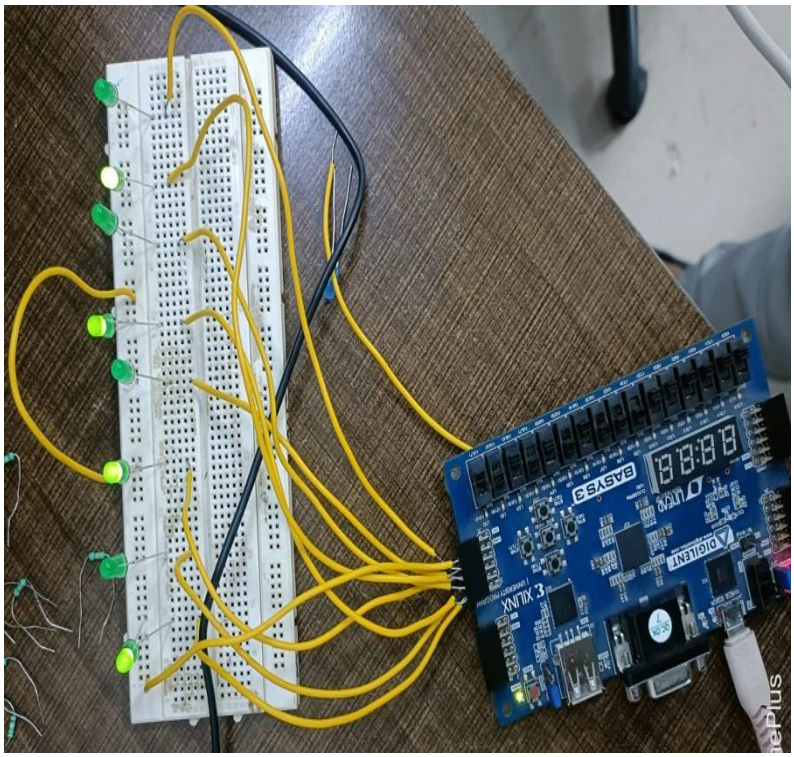

Figure 3.8 LED controlled by FPGA

3.4. Unit Cell Model of the RIS:

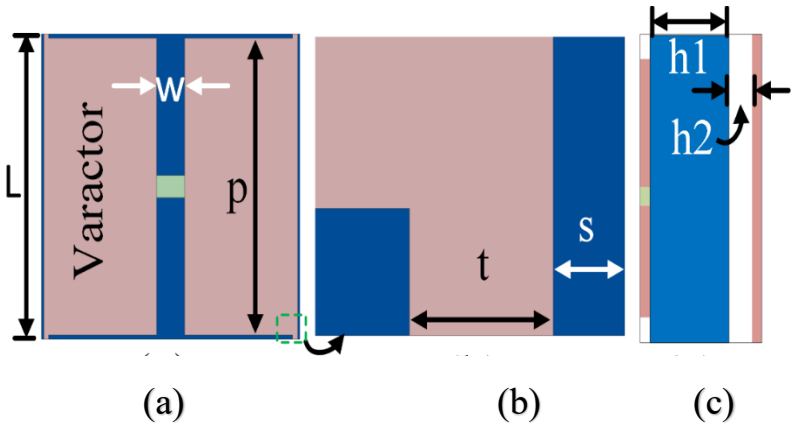

Figure 3.9 Unit cell of geometry of the proposed RIS: (a) top view, (b) enlarged view of biasing lines, and (c) side view. The dimensions are: L = 11 mm, P = 10.7 mm, w = 1.2 mm, s = 0.1 mm, t = 0.2 mm, h1 = 1.6 mm, and h2 = 0.8 mm

Fig. 3.9 illustrates the unit cell configuration of the proposed RIS design, which consists of a top metallic layer, a dielectric substrate, an intermediate air gap, and a bottom ground plane. A varactor diode is integrated between two identical rectangular patches in the top metallic layer, while biasing lines at the edges of each patch to enable voltage regulation. The dielectric substrate is made of FR4, with a relative permittivity of 4.4 and a loss tangent of 0.02, while the ground plane is fabricated from copper with a thickness of 0.035mm. The BB857-02V varactor diode is selected,

3.4.1. Equivalent circuit modelling:

To further investigate the EM operation of the geometry, an equivalent circuit model is formulated, as illustrated in Fig. 3.10. The circuit is structured as a combination of a Rg-Lg-Cg circuit in series with the diode parameters, where Rg and Lg correspond to the top metallic patch and Cg is the gap capacitance between the successive unit cells. The varactor diode is characterized by a tunable capacitance (C_V) and a parasitic resistance (R_S). The dielectric substrate and the air spacer are modeled as transmission line sections with electrical length h_1 and h_2, respectively, corresponding to the transmission line impedances of Zd and Za, whereas the ground plane is replaced with a short-circuit line. Two different operating states are considered with capacitance values of 0.77 pF and 1.55 pF, and the circuit parameter values are determined using the curve tracking method in ADS software

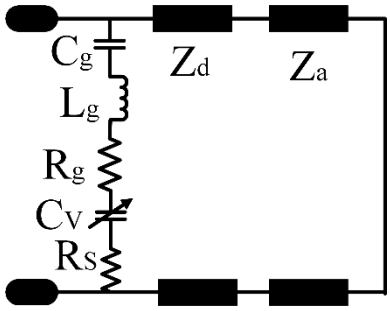

Figure 3.10 Equivalent circuit model of the proposed RIS unit cell

3.4.2. Simulation Result of unit cell:

The unit cell is studied using periodic boundary conditions in Ansys HFSS, and its electromagnetic (EM) responses are analyzed by varying the junction parameter capacitance across the diode. The topology has initially been designed without considering the air gap, however, the same has incurred considerable power dissipations and uneven phase distributions, as depicted in Figs. 3.11(a) and 3.11(b), respectively. To mitigate this issue, an air gap is introduced between the substrate and the ground plane. This not only improves the reflection coefficient (S_{11}) amplitude from -4 dB to -2.5 dB at the operating frequency 3.6 GHz, the S_{11} phase becomes evenly distributed for different values of capacitance, as shown in Figs. 3.11(c) and 3.11(d). Among them, two states are considered corresponding to the capacitance value of 0.77 pF and 1.55 pF, which exhibit S_{11} phases of +120° and -60°, respectively, thereby constituting a phase difference of 180°, required for designing the RIS geometry.

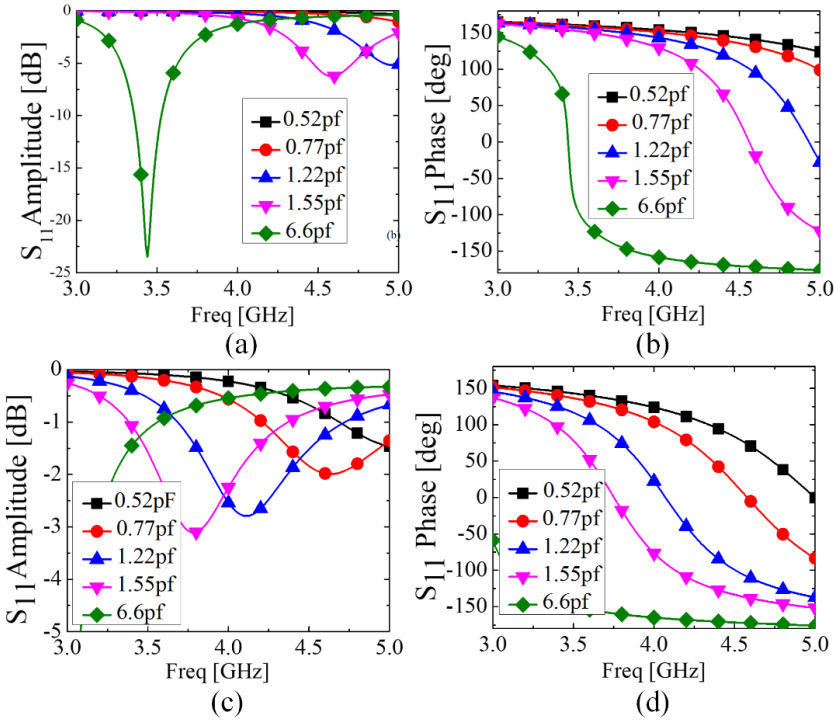

Figure 3.11 Simulated S_{11} responses of the proposed unit cell geometry for different conditions: without the air gap: (a) amplitude, (b) phase, and with air gap: (c) amplitude, (d) phase.

3.4.3 Comparison between calculated and simulated Result:

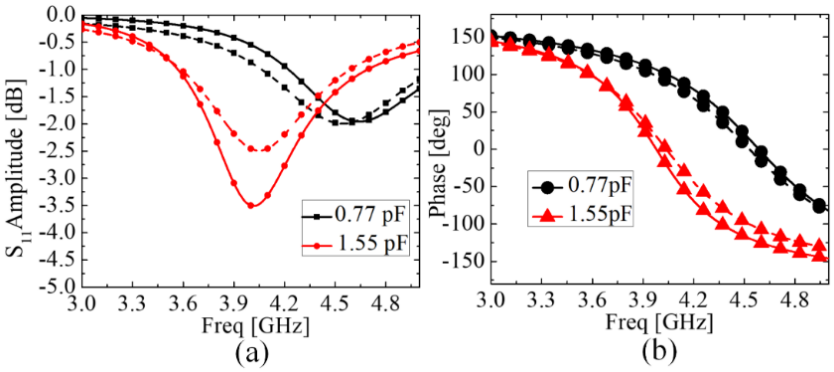

Figure 3.12 Comparison between calculated and simulated S_{11} responses for different operating states: (a) amplitude, and (b) phase. The dashed line represents the ADS results, and the solid lines represent HFSS results

Fig. 3.12 shows how the reflection coefficient (S_{11}) varies with frequency for two different capacitance values—0.77 pF and 1.55 pF—across both amplitude and phase. In Fig. 3.12(a), we observe the amplitude of S_{11}, where both calculated (dashed lines from ADS) and simulated (solid lines from HFSS) results align closely. The deeper the dip in the curve, the better the impedance matching. Fig. 3.12(b) shows the phase response of S_{11} over frequency. It can be clearly seen that changing the capacitance value shifts both amplitude and phase characteristics significantly. This demonstrates how tuning components like varactors or pin diodes can reconfigure a surface's electromagnetic behavior. The strong match between ADS and HFSS results also validates the accuracy of the design approach.

3.5. Simulation setup:

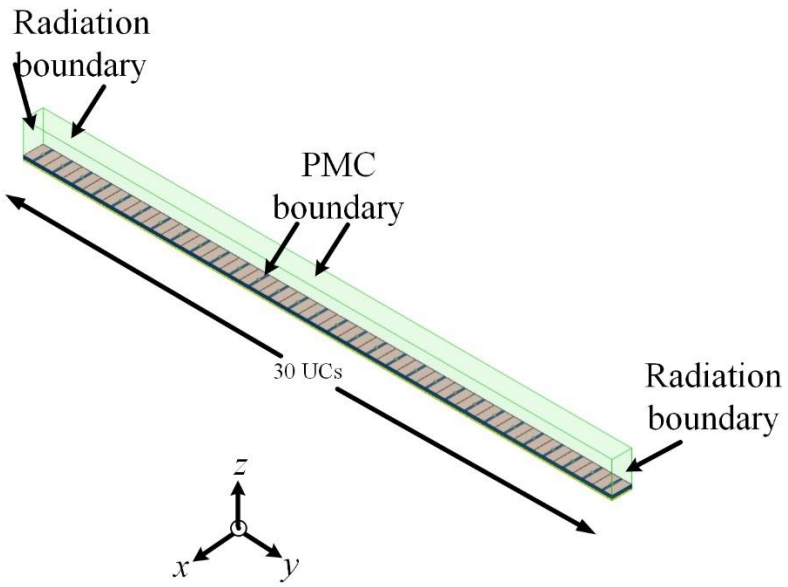

Figure 3.13 Simulation set up of the proposed RIS unit cell array

To demonstrate the performance, a single array of 30-unit cells is considered in the y-direction with periodic boundary conditions (PMC boundary) applied in ±x directions and a plane wave impinged from +z-direction. The open boundary (radiation boundary) conditions are applied in ±y-directions, as illustrated in Fig. 3.13. This setup mimics identical unit cells arranged in the x-direction, while different unit cells are placed along the y-direction. By applying different bias voltages across the unit cells in the y-direction, a desired phase profile can be generated, resulting in the beamforming operation. Such configurations provide the beamforming operation in the YZ plane ($-\infty < y < +\infty$; $0 < z < \infty$).

Table 1 Beam steering Operation of Proposed RIS

Beam Steering Angle	**Phase Pattern**
0°	000000000000000000000000000000
15°	011111111111110000000000000111
30°	011111000000011111111000000011
45°	011110000011111000001111100001
±30°	111111000000111111000000111111
30°, -20°	011111100000001111110000000000
30°, -15°	011111100000001111111111111000
20°, -10°	011111111100000000001111111111

3.5.1 Simulation result of setup:

A 1-bit phase coding scheme is employed in the metasurface, where the unit cells are assigned binary states with a 180^{o} phase shift, where 0 and 1 are assigned to the states corresponding to the capacitance values of 0.77 and 1.55 pF, respectively. Thereafter, different phase profiles are generated for different beamforming operations, based on the generalized Snell's law, and subsequently assigned to the unit cells in the array geometry. Table I summarizes the phase encoding patterns for different beam steering angles, corresponding to a normally incident EM wave. The beamforming characteristics demonstrate the deflection achieved at various target angles. Initially, the structure is configured to obtain a beam steering operation for 0°, 15°, 30°, and -45° directions with different sets of phase profiles, as shown in Fig. 3.14. Since the structure is designed based on 1-bit configuration, the limited resolution of phase states (only two-phase states, e.g. 0° and 180°) leads to the generation of symmetric radiation pattern in the far field. This limitation underscores the trade-off between hardware simplicity and beamforming precision in low-resolution RIS architectures. Furthermore, the geometry supports beam-splitting functionality, enabling symmetric beam splitting ±30°, as depicted in Fig. 3.15. In addition, the geometry can be used for multi-user systems, where the beam can be non-uniformly directed at two different directions with unequal amplitudes, as observed in Fig. 3.16. 0 state and 1 state represent unit cells with diode capacitance value of 0.77 pF and 1.55 pF, respectively.

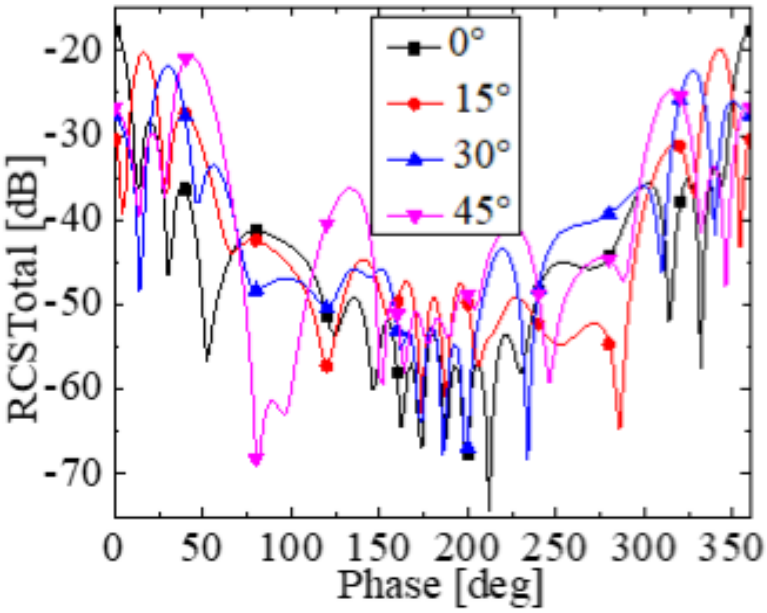

Figure 3.14 Radar cross section (RCS) of the RIS for single-user beam steering

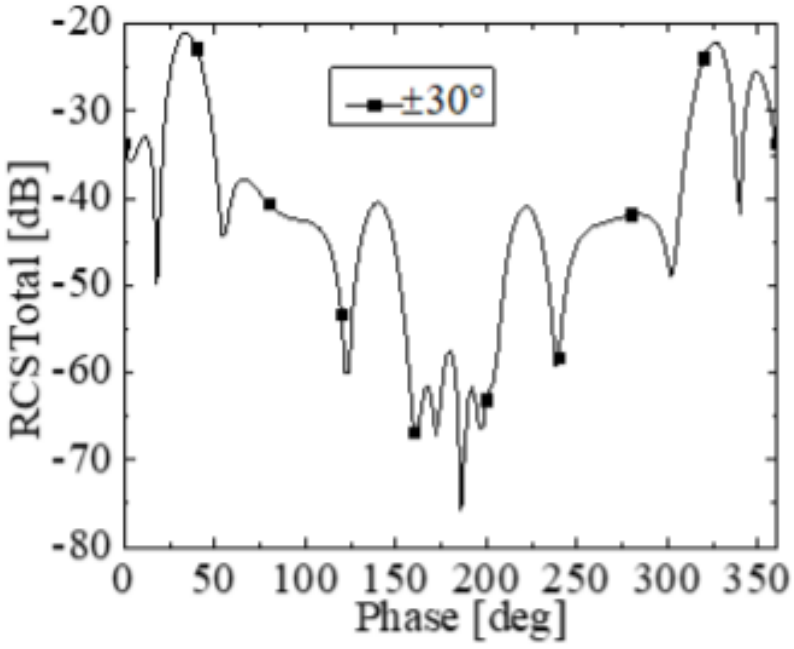

Figure 3.15 Radar cross section (RCS) of the RIS for beam splitting

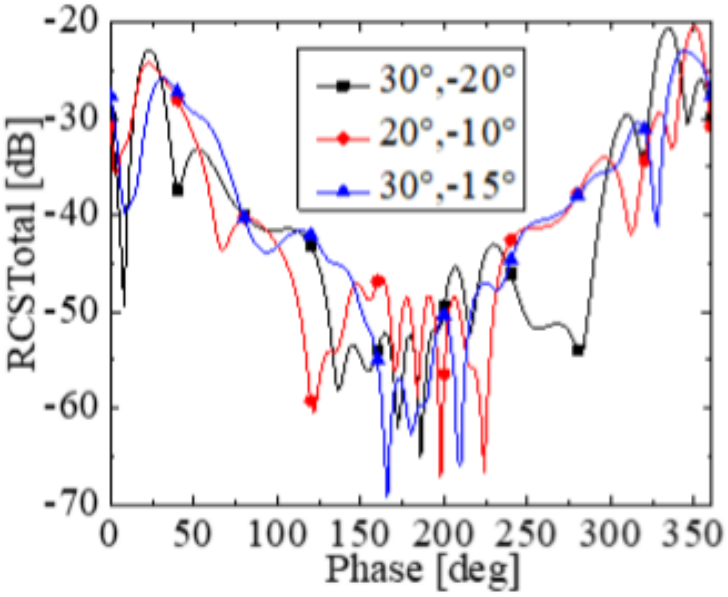

Figure 3.16 Radar cross section (RCS) of the RIS for multi-user beam steering

Chapter 4

Fabrication and Measurement

4.1. Measurement setup:

Figure 4.1 Experiment setup for RIS measurement

To experimentally validate the beamforming capabilities the proposed RIS, a two-dimensional prototype consisting of 30 × 30-unit cells has been fabricated. The diodes mounted in the unit cells over a single column are regulated by a voltage source, whereas unit cells placed in different rows are biased with different voltages based on the desired phase profile. A complete test bed has been setup for measuring the performance of the prototype, which consists of a host computer, an URSP B210 kit from National Instruments (NI), and a horn antenna in the transmitting side. The host computer plays a crucial role by interfacing with the USRP and facilitating the generation of modulated signal, which has subsequently been transmitted as a RF source through the horn antenna. The receiving side consists of another horn antenna

connected to a spectrum analyzer, such that the re-radiated signal can be observed in the analyzer. Based on the desired beam direction, the antennas are positioned accordingly, effectively emulating a dynamic environment to observe the effect of the RIS on signal propagation.

During the measurement, different test cases are considered based on the incident and reflected angle, and the bias voltages across the unit cells have been applied accordingly. The signal from the prototype has first been measured, and then the response is recorded for a copper plate of the same size. The comparison between these two responses cancels out the propagation loss and other environment effects, while exhibiting the improvement of signal power with respect to the metal plate. The signal has been measured for single-user case, where the reflected beam is directed at 30° and 45° in two separate scenarios, as depicted in Fig. 4.2 and 4.3, respectively, for a normally incident wave. An improvement in the power level of above 18 dB with respect to the copper plate is observed for both cases. Next, the geometry is configured for beam splitting case, where the re-radiated beam is equally splits at +30° and -30°. Similar power levels are observed at these two directions in Fig. 4.4, confirming the splitting operation of the geometry. Finally, the signal is divided unequally in two directions, one beam at -15° and other at +30°, and the received signals are found similar to each other, as shown in Fig. 4.5. Furthermore, all these cases confirm the enhancement of the signal during the presence of RIS. In addition, a reduction in the BER and increase in the SE are simultaneously observed in the fabricated RIS.

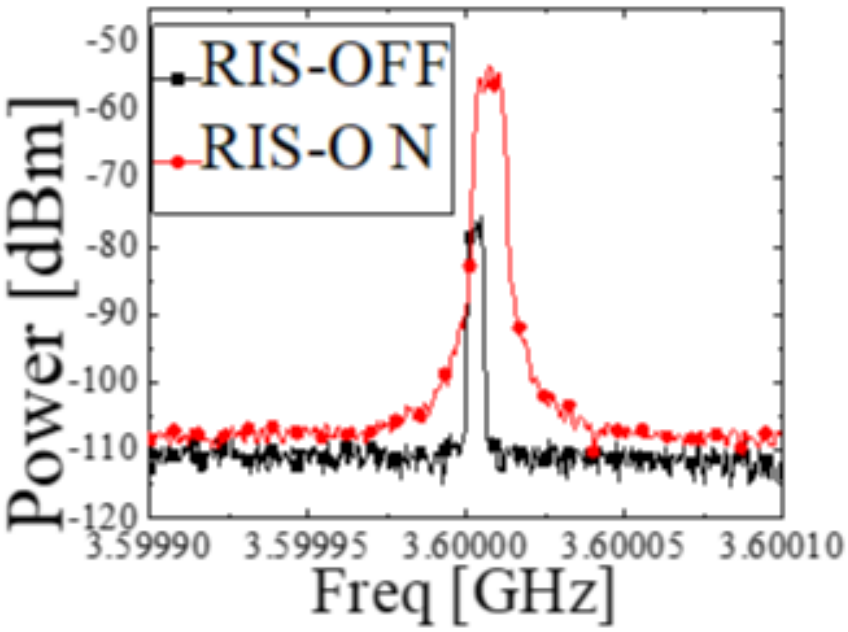

Figure 4.2 Comparison of power level between the RIS structure (RIS-ON) and a similar size metal plate (RIS OFF), when the signal is incident at 0° and reflected at 30

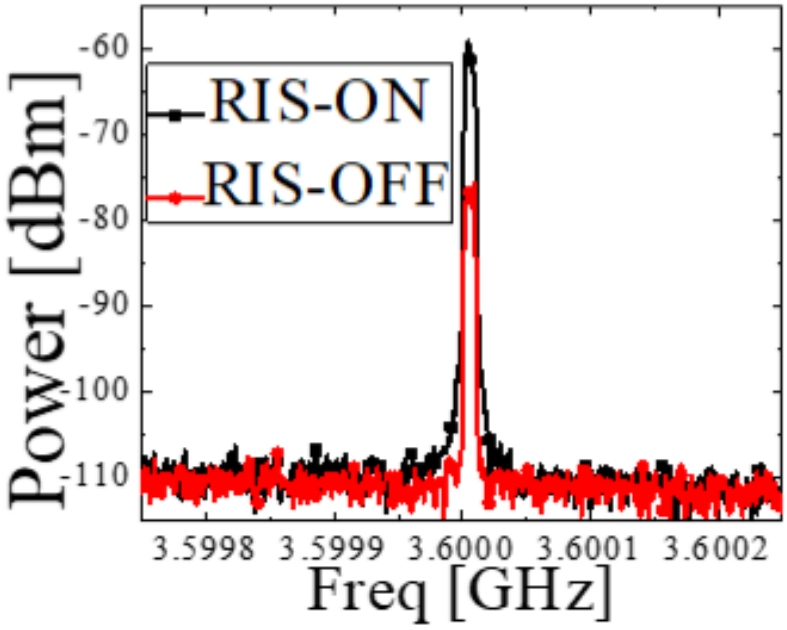

Figure 4.3 Comparison of power level between the RIS structure (RISON) and a similar size metal plate (RIS-OFF), when the signal is incident at 0° and reflected at 45°

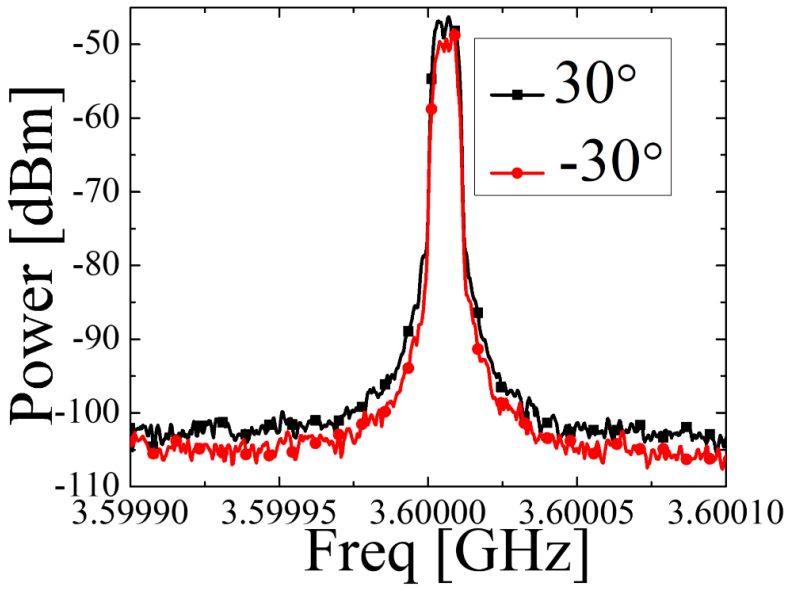

Figure 4.4 Power levels of two reflected beams directed at +30° and -30°

.

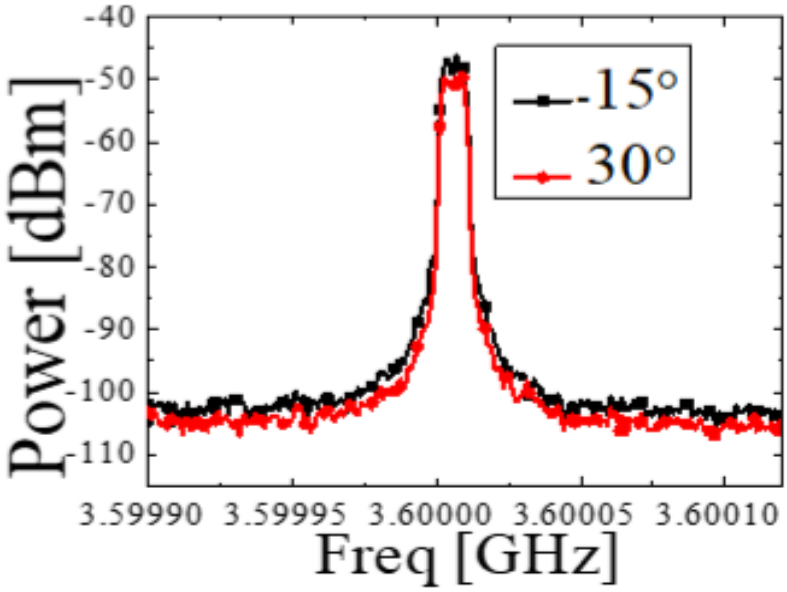

Figure 4.5 Power levels of two reflected beams directed at +30° and -15° in a multi-user environment

4.2. Reciprocity Test:

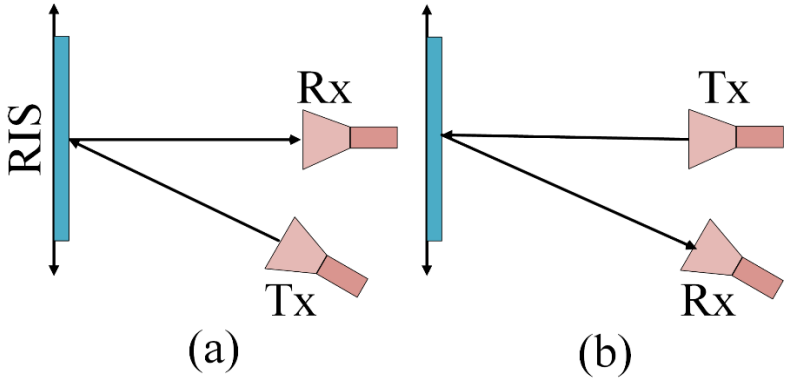

Figure 4.6. Reciprocity test: (a) Case 1, and (b) Case 2

An experimental verification has also been carried out to test the reciprocity feature of the fabricated RIS prototype by evaluating its reflection properties under identical forward and reverse propagation conditions. In the first case (Case 1), the transmitting horn antenna is placed at +30°, while the receiving antenna is placed at 0° angle. In the next case, the roles of transmitter and receiver are interchanged, and the corresponding measurement has been recorded. The setups are illustrated in Fig. 4.6. The experimental results are presented in Fig. 4.7 and it is observed that the RIS maintains the reciprocity condition, validating its feasibility for symmetric wireless channel modeling.

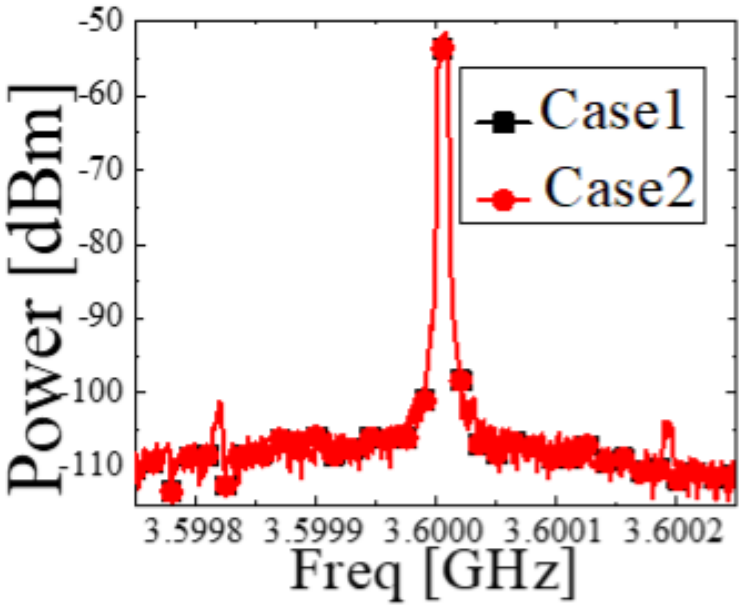

Figure 17. Power levels of reflected beams directed at 30°, generated during Cases 1 and 2

Chapter 5

Conclusion and Future Scopes

5.1. Conclusion:

This paper introduces a novel RIS geometry designed to support advanced functionalities such as single-user and dual-user beam steering, along with beam splitting capabilities. The proposed RIS architecture leverages a 1-bit phase coding technique, implemented through the integration of varactor diodes onto the surface structure. This approach allows dynamic control over the phase response of individual RIS elements, enabling effective redirection and manipulation of electromagnetic waves. One of the key advantages of the design is its wide angular coverage, which ensures efficient beam steering over a broad range of directions.

The proposed RIS geometry has been rigorously analysed using an equivalent circuit model that offers valuable insight into the underlying electrical behaviour of the unit cell structure. To validate the theoretical findings, comprehensive full-wave simulations have been conducted, alongside experimental measurements using a fabricated prototype. The experimental results confirm the RIS's capability to perform beam steering and beam splitting with high accuracy and reliability. Furthermore, the system demonstrates strong performance in both single- and dual-user scenarios, highlighting its versatility in next-generation wireless communication systems.

To evaluate its relative performance, a detailed comparison has been presented in Table II, where the proposed design is benchmarked against several existing RIS configurations reported in the literature.

The results clearly indicate improvements in angular resolution, operational bandwidth, and beam control precision. These enhancements position the proposed RIS as a highly promising candidate for integration into future wireless technologies such as 6G, smart environments, and massive MIMO systems.

Table 2 COMPARISON WITH EXISTING RIS GEOMETRIES

Reference	**Unit cell design**	**Unit cell size**	**Frequency (GHz)**	**Functionality**
[8]	Hybrid RIS	0.25λ × 0.25λ	2.5	No steering
[9]	1-bit RIS	0.38λ × 0.35λ	5.8	No steering
[10]	1-bit RIS	0.5λ × 0.5λ	12.5	No steering
[11]	Passive RIS	0.16λ × 0.16λ	5.8	no steering/no steering
[12]	3-bit RIS	0.27λ× 0.27λ	3.18	No steering
[13]	1-bit RIS	0.55λ × 0.55λ	5	No dual beam steering
This work	**1-bit RIS**	**0.13λ × 0.13λ**	**3.6**	**Single-, dual-user steering/ splitting**

5.2. Future Score:

Reconfigurable Intelligent Surfaces (RIS) have shown great potential in improving wireless communication by intelligently controlling electromagnetic waves. One major future application of RIS is in the development of 6G communication systems. RIS can help in achieving ultra-high data rates, low latency, and energy-efficient communication. With the rising demand for smart connectivity in applications like autonomous vehicles, remote surgery, and augmented reality, RIS will be a key enabling technology to meet those requirements by dynamically shaping and redirecting wireless signals.

Another promising area where RIS can be applied is in smart indoor environments and smart cities. RIS can be embedded into walls, ceilings, and objects to improve wireless coverage in areas with poor signal reception, like basements or high-rise buildings. This can reduce the need for multiple routers or base stations and ensure consistent high-quality wireless signals everywhere. Future developments can make RIS more compact, cost-effective, and easier to install in everyday infrastructure, making them a practical solution for urban and residential connectivity.

RIS can also play a vital role in satellite and UAV-based communications. Traditional communication with moving objects like drones or satellites suffers from weak and unstable signals. With RIS, beam steering and signal focusing can be dynamically adjusted in real-time to maintain strong links, even when devices are in motion. This makes RIS a good fit for disaster management, rural connectivity, and military communications where traditional setups are often not feasible

.

Lastly, the future of RIS lies in its integration with AI and machine learning. Intelligent algorithms can control the phase shifts of each RIS unit cell based on the environment, user position, and channel conditions. This makes the system self-adaptive and capable of learning over time to optimize performance. As research progresses, RIS is expected to become more autonomous and capable of real-time decision-making, transforming the way we manage wireless networks and pushing the limits of communication technology.

References

[1] E. Basar, *et al.*, "Wireless communications through reconfigurable intelligent surfaces," *IEEE Access*, vol. 7, pp. 116753-116773, 2019.

[2] M. Di Renzo, *et al.*, "Smart radio environments empowered by reconfigurable intelligent surfaces: how it works, state of research, and the road ahead*," IEEE Journal on Selected Areas in Communications*, vol. 38, no. 11, pp. 2450-2525, Nov. 2020.

[3] A. Taha, M. Alrabeiah and A. Alkhateeb, "Enabling large intelligent surfaces with compressive sensing and deep learning", *IEEE Access*, vol. 9, pp. 44304-44321, Mar. 2021.

[4] J. Y. Dai, *et al.*, "Wireless communications through a simplified architecture based on time-domain digital coding metasurface", *Adv. Mater. Technol.*, vol. 4, no. 7, pp. 1-8, Jul. 2019.

[5] W. Tang, *et al.*, "Programmable metasurface-based RF chain-free 8PSK wireless transmitter", *Electron. Lett.*, vol. 55, no. 7, pp. 417-420, 2019.

[6] T. J. Cui, M. Q. Qi, X. Wan, J. Zhao, and Q. Cheng, "Coding metamaterials digital metamaterials and programmable metamaterials", *Light Sci. Appl*., vol. 3, no. 10, pp. e218, Oct. 2014.

[7] X. Wan, M. Qi, T. Chen, and T. Cui, "Field-programmable beam reconfiguring based on digitally-controlled coding metasurface", *Sci. Rep*., vol. 6, Feb. 2016.

[8] Y. Chandrakapure, R. Malleboina, A. Kumar and D. Sarkar, "A multi-state reconfigurable intelligent surface based on

anomalous reflectors for communication and radar applications," *2024 National Conference on Communications (NCC)*, Chennai, India, 2024.

[9] X. Pei, *et al.*, "RIS-aided wireless communications: prototyping, adaptive beamforming, and indoor/outdoor field trials," *IEEE Transactions on Communications*, vol. 69, no. 12, pp. 8627-8640, Dec. 2021.

[10] H. Yang, *et al.*, "A 1-bit 10×10 reconfigurable reflectarray antenna: design, optimization, and experiment," *IEEE Transactions on Antennas and Propagation*, vol. 64, no. 6, pp. 2246-2254, 2016.

[11] R. Malleboina, J. C. Dash, and D. Sarkar, "Design of anomalous reflectors by phase gradient unit cell-based digitally coded metasurface," *IEEE Antennas and Wireless Propagation Letters*, vol. 22, no. 9, pp. 2305-2309, Sept. 2023

[12] J. C. Liang, *et al.*, "An angle-insensitive 3-Bit reconfigurable intelligent surface," *IEEE Transactions on Antennas and Propagation*, vol. 70, no. 10, pp. 8798-8808, Oct. 2022.

[13] J. Han, L. Li, G. Liu, Z. Wu, and Y. Shi, "A wideband 1 bit 12 × 12 reconfigurable beam-scanning reflectarray: design, fabrication, and measurement," *IEEE Antennas and Wireless Propagation Letters*, vol. 18, no. 6, pp. 1268-1272, June 2019.

[14] G. C. Trichopoulos, *et al.*, "Design and Evaluation of Reconfigurable Intelligent Surfaces in Real-World Environment," *IEEE Open Journal of the Communications Society*, vol. 3, pp. 462-474, 2022.

[15] D. Fei, *et al.*, "Research and experimental verification of reconfigurable intelligent surface in indoor coverage enhancement," 电子与信息学报, vol. 44, no. 7, pp. 1-8, 2022.

[16] A. Sayanskiy, *et al.*, "A 2D-programmable and scalable reconfigurable intelligent surface remotely controlled via digital infrared code," *IEEE Transactions on Antennas and Propagation*, vol. 71, no. 1, pp. 570-580, Jan. 2023.

[17] J. Rains, *et. al.*, "High resolution programmable scattering for wireless coverage enhancement: an indoor field trial campaign," *IEEE Transactions on Antennas and Propagation*, vol. 71, no. 1, pp. 518-530, Jan. 2023.

[18] R. Liu, J. Dou, P. Li, J. Wu, and Y. Cui, "Simulation and field trial results of reconfigurable intelligent surfaces in 5G networks," *IEEE Access*, vol. 10, pp. 122786-122795, 2022.

[19] M. Cui, Z. Wu, Y. Chen, S. Xu, F. Yang, and L. Dai, "Demo: low-power communications based on RIS and AI for 6G," in *2022 IEEE International Conference on Communications Workshops* (*ICC Workshops*), 2022, pp. 1-2.

[20] J. B. Gros, V. Popov, M. A. Odit, V. Lenets, and G. Lerosey, "A reconfigurable intelligent surface at mm-wave based on a binary phase tunable metasurface," *IEEE Open Journal of the Communications Society*, vol. 2, pp. 1055-1064, 2021.

[21] E. G. Larsson, "Massive MIMO for 5G: overview and the road ahead," in *2017 51st Annual Conference on Information Sciences and Systems* (*CISS*), 2017, pp. 1-1.

[22] A. Amiri, M. Angjelichinoski, E. d. Carvalho, and R. W. Heath, "Extremely large aperture massive MIMO: low complexity

receiver architectures," in *2018 IEEE Globecom Workshops* (GC Wkshps), 2018, pp. 1-6.

[23] J. Y. Dai, *et al.*, "Realization of multi-modulation schemes for wireless communication by time-domain digital coding metasurface," *IEEE Transactions on Antennas and Propagation*, Article vol. 68, no. 3, pp. 1618-1627, 2020

[24] N. M. Tran, M. M. Amri, J. H. Park, D. I. Kim, and K. W. Choi, "Multifocus techniques for reconfigurable intelligent surface-aided wireless power transfer: theory to experiment," *IEEE Internet of Things Journal*, vol. 9, no. 18, pp. 17157-17171, 2022.

[25] R. Bajaj, S. L. Ranaweera, and D. P. Agrawal, "GPS: location-tracking technology," *Computer*, vol. 35, no. 4, pp. 92-94, 2002.

[26] J. Bassey, D. Adesina, X. Li, L. Qian, A. Aved, and T. Kroecker, "Intrusion detection for IoT devices based on RF fingerprinting using deep learning," in *2019 fourth international conference on fog and mobile edge computing* (*FMEC*), 2019, pp. 98-104.

[27] S. A. Shah and F. Fioranelli, "RF sensing technologies for assisted daily living in healthcare: a comprehensive review," *IEEE Aerospace and Electronic Systems Magazine*, vol. 34, no. 11, pp. 26-44, 2019

[28] A. Tundis, H. Kaleem, and M. Mühlhäuser, "Detecting and tracking criminals in the real world through an IoT-based system," (in eng), *Sensors*, vol. 20, no. 13, p. 3795, 2020.

[29] L. N. Kandel and S. Yu, "Indoor localization using commodity Wi-Fi APs: techniques and challenges," in *2019 International Conference on Computing, Networking and Communications* (*ICNC*), 2019, pp. 526-530.

[30] H. Zhang, H. Zhang, B. Di, K. Bian, Z. Han, and L. Song, "MetaLocalization: reconfigurable intelligent surface aided multi-user wireless indoor localization," *IEEE Transactions on Wireless Communications*, Article vol. 20, no. 12, pp. 7743-7757, 2021

[31] G. Zhang, D. Zhang, Y. He, J. Chen, F. Zhou, and Y. Chen, "Multi-person passive WiFi indoor localization with intelligent reflecting surface," *IEEE Transactions on Wireless Communications*, vol. 22, no. 10, pp. 6534-6546, Oct. 2023.

[32] W. Taylor, *et al.*, "An intelligent noninvasive real-time human activity recognition system for next-generation healthcare," *Sensors*, vol. 20, no. 9, 2020.

[33] H. F. Thariq Ahmed, H. Ahmad, and A. C.V, "Device free human gesture recognition using Wi-Fi CSI: A survey," *Engineering Applications of Artificial Intelligence*, Article vol. 87, 2020.

[34] E. Cardillo and A. Caddemi, "A review on biomedical mimo radars for vital sign detection and human localization," *Electronics*, vol. 9, no. 9, pp. 1-15, 2020.

[35] M. Usman, *et al.*, "Intelligent wireless walls for contactless in-home monitoring," *Light: Science & Applications*, vol. 11, no. 1, 2022